Utilization of Lignin and Lignosulfonate from Oil Palm Empty Fruit Bunches as Filler in PVDF Proton Exchange Membrane Fuel Cell

Nala Ridhwanul Mu'izzah, Pinka Zuhdiana Hapsari, Nabila Putri Aulia, Dian Wahyu Tri Wulansari, Fauziyah Azhari, and Edi Pramono*

Department of Chemistry, Faculty of Mathematics and Natural Sciences, Universitas Sebelas Maret, Jl. Ir. Sutami 36A, Kentingan, Surakarta 57126, Indonesia

* ***Corresponding author:***

email: edi.pramono.uns@staff.uns.ac.id

Received: January 26, 2023
Accepted: June 19, 2023

DOI: 10.22146/ijc.81750

Abstract: *A study on the polyvinylidene fluoride (PVDF) membrane using lignin and lignosulfonate oil palm empty fruit bunch (OPEFB) fillers have been carried out. This study aims to determine the additional effect of lignin and lignosulfonate on PVDF membrane. Lignin sulfonation has a good result proven by Fourier transform infrared spectra with a peak at 1192 cm^{-1} which indicates sulfonate group. The sulfonation degree was increased by 8.9% for lignosulfonate. The membrane was prepared by the phase inversion method. Data present that all the membranes have an asymmetric structure with finger-like and sponge-like pores. Good thermal stability indicated by thermal gravimetric analysis showed degradation at 432 °C. The mechanical properties of the membrane decrease with the addition of filler. From the X-ray diffraction, peaks appeared at 18.39°, 21.35°, and 23.75° for all the membranes indicating of α and β phases. Lignin and lignosulfonate increased membrane hydrophilicity and water uptake. The presence of the sulfonate group increases the ionic exchange capacity and ionic conductivity up to 2.78 mmol/g and 9.95 × 10^{-5} S/cm, respectively, for 5% lignosulfonate addition. Thus, PVDF/lignosulfonate has the potential as a polymer electrolyte membrane.*

Keywords: *lignin; lignosulfonate; OPEFB; polymer electrolyte membrane; PVDF*

■ INTRODUCTION

A fuel cell is an electrochemical device in which chemical energy is directly converted into electrical energy [1]. Fuel cells are one of the alternative energy production technologies [2], where hydrogen is used as an energy source [3]. Hydrogen can produce high energy and lower calorific value than hydrocarbon-based fossil fuels, making it more efficient [4] and environmentally friendly [2]. In addition, hydrogen is ideally used for fuel cells due to its rapid electrochemical reaction kinetics and the absence of exhaust gases since the only by-product of the reaction is water [4]. The essential elements of a fuel cell are the positive electrode (cathode), the negative electrode (anode), and the electrolyte membrane [4-5].

The perfluorosulfonic acid polymer (Nafion®) has high ionic conductivity, mechanical and chemical stability at lower temperatures [6]. Nafion® also has a multiphase structure, namely the hydrophobic phase as the continuous phase and the sulfonic acid group as the hydrophilic phase. The continuous hydrophobic phase is helpful for the structural integrity of the membrane, and the hydrophilic phase acts as a reservoir of water [7]. However, Nafion® is expensive and challenging to synthesize [8], so researchers are looking for another alternative to be developed. One alternative polymer that can be used is polyvinylidene fluoride (PVDF), which has good mechanical properties, thermal stability, and chemical resistance [9]. Even so, PVDF has limitations due to its low conductivity [10], which requires to be modified.

Physical modification, such as mixing with other components, can be used to improve PVDF membrane performance [11]. Lignin has the potential to modify PVDF membranes. Lignin has some polar groups in its structure, especially the hydroxyl group [12], which can be an active modification center [13]. Lignin has

advantages, including high carbon content, good thermal stability, biodegradability, good antioxidant activity, and good mechanical properties. With modification by sulfonation reaction, lignin has hydrophilic properties [7-8] and has the potential to be used as a polymer electrolyte. The presence of a sulfonate group facilitated the transfer of protons [14], increasing the conductivity of the PVDF membrane. Lignin is also an abundant biopolymer and is a by-product of cellulose extraction [15] from various biomass such as oil palm empty fruit bunches (OPEFB). In Indonesia, around 7 million tons of OPEFB are estimated to be produced annually [16]. Previous research reports that the effect of lignin coating on PVDF membranes showed promising results on membrane surface properties with increased hydrophilicity values [17]. Lignin was also increasing the ionic exchange capacity of poly (ether ether ketone) (SPEEK) membranes [18]. However, the blending of lignin and lignosulfonate in PVDF as polymer electrolyte membranes has never been studied. This research determines the effect of lignin and lignosulfonate on morphology, matrix structure, hydrophilicity, thermal, mechanical, and electrolyte properties.

■ EXPERIMENTAL SECTION

Materials

The materials used are oil empty palm fruit bunches (OPEFB) obtained from Polytech Institute Technology Indonesia. PVDF Solef 1010 pellets were bought from Solvay. Sodium hydroxide (NaOH), sulfuric acid (H_2SO_4), hydrochloric acid (HCl), dimethylacetamide (DMAC), sodium chloride (NaCl), and sodium sulfite (Na_2SO_3) in analytical grades were purchased from Merck.

Instrumentation

The instruments used in this study are Fourier transform infrared (FTIR, Shimadzu IR Prestige-21), scanning electron microscope (SEM, Jeol JCM-7000), simultaneous thermal analyzer (STA, LINSEIS PT1600), X-ray diffractogram (XRD, D8 Advance Bruker Germany), attenuated total reflection-Fourier transform infrared (ATR-FTIR, Agilent Cary 600), and electrochemical impedance spectroscopy (EIS, EUGOL U2826).

Procedure

Lignin isolation from OPEFB

Extraction was performed by refluxing OPEFB using a 0.5 M NaOH solution in a ratio of 1:20 (w/v) for 2 h at 90–100 °C. The results were filtered so that black liquor was obtained. Black liquor was acidified using H_2SO_4 1 M to reach pH 2 and precipitated for at least 8 h. The precipitate was filtered and dried at room temperature.

Sulfonation of lignin

Sulfonation followed the procedure of previous research [19] with modifications. Lignin was mixed with Na_2SO_3 and distilled water with a ratio of 2:1:20. The mixture was stirred for 4 h at 80 °C. The mixture was evaporated in the oven at 60 °C for 6 h. The resulting lignosulfonate is grounded and sifted using a 200-size mesh before use.

Sulfonation degree

The sulfonation degree was calculated using conductometric titration based on previous research [20]. First, 0.1 g of lignin and lignosulfonate was diluted in 60 mL NaOH 0.01 M through ultra-sonification for 10 min and pH was adjusted to 2.8 by adding HCl 0.1 M to ensure all the sulfonated groups were protonated. The dispersion was purged with nitrogen for 20 min and titrated using NaOH 0.01 M. The change in conductance was observed. The value of the sulfonation degree was computed using Eq. (1).

$$SD = \frac{(V_{NaOH} \times C_{NaOH}) - (V_{HCl} \times C_{HCl})}{w} \quad (1)$$

where SD is sulfonation degree (mmol/g) and w is weight of lignin or lignosulfonate (g).

Membrane fabrication

PVDF, PVDF/Lignin (PL), and PVDF/Lignosulfonate (PLS) membranes were prepared using the phase inversion method followed by previous research [21]. The total mass of the casting solution (dope) was 12 g with a composition of lignin and lignosulfonate varied to 1, 3, and 5% by weight of PVDF. The composition of the membranes is shown in Table 1. Dope was made by dissolving lignin or lignosulfonate in DMAC and then supplemented with PVDF. The dope

Table 1. Membrane composition

Membrane	Composition*			
	PVDF (% w/w)	Lignin (% w/w)	Lignosulphonate (% w/w)	DMAC
PVDF	18	-	-	82
PL-1	18	1	-	82
PL-3	18	3	-	82
PL-5	18	5	-	82
PLS-1	18	-	1	82
PLS-3	18	-	3	82
PLS-5	18	-	5	82

*The composition of Lignin and lignosulfonate is calculated based on PVDF weight

was stirred for 24 h at 50–60 °C, cast on glass with a thickness regulator of 130 μm and directly put into a coagulant bath filled with water.

Characterization

Isolation and sulfonated lignin were characterized by FTIR. Sample scanned 48× with resolution 1 cm^{-1} at range 4000–400 cm^{-1} using KBr pellet.

Membrane surface and cross-section morphology were analyzed using SEM. The membrane was observed with a magnification of 10,000× for surface morphology and 1,000× for cross-section.

Membrane thermal analysis was conducted using the STA with an alumina crucible dish and an air atmosphere. Membranes were burned with a heating rate of 10°/min (dpm) in the temperature range of 25–900 °C. Further analysis was performed using Origin software.

The mechanical properties of the membrane were characterized using Inston MOD 1026 tensile strength tester. Membrane with the dimensions of 6×0.5 cm^2 tested at the speed of 80 mm/min, pinch distance of 20 mm and weight of 500 g. The mechanical properties were calculated using Eq. (2-4);

$$\sigma = \frac{F}{A} \quad (2)$$

$$\varepsilon = \frac{\Delta l}{l} \times 100\% \quad (3)$$

$$\gamma = \frac{\sigma}{\varepsilon} \quad (4)$$

where σ is tensile strength (MPa), F is force (kg/ms^2); A is surface area (cm^2), ε is elongation (%), Δl is change in length (mm), l is original length (mm), and γ is Young Modulus (MPa).

Membrane structure was characterized using XRD. The membrane was cut with dimensions of 2×2 cm^2 and dried at 60 °C for 24 h. The membrane was scanned at 2θ 10–90°, and the data was processed using Origin software.

ATR-FTIR was used to identify the α and β phases related to membrane hydrophilicity. The analysis is carried out at a wavelength of 4000–400 cm^{-1}, and the β fraction was computed using Eq. (5) [22].

$$F(\beta) = \frac{A\beta}{A\beta + 1.26A\alpha} \times 100\% \quad (5)$$

where Aα and Aβ were the absorbances at peaks of 762 and 840 cm^{-1} corresponding to the α and β phases, respectively.

Membrane hydrophilicity was determined by measuring the water contact angle (WCA). The measurement was carried out by calculating the angle of water drops on the membrane surface. The images were taken using a 48-megapixel HP camera lens with a magnification of 5×. Images were analyzed using ImageJ software with a contact angle plugin.

The water uptake membrane was analyzed using the gravimetric method. The wet membrane (W_w) was weighed and dried at 60 °C for 24 h. The dry membrane (W_d) was weighed again, and the water uptake was determined through Eq. (6) [18].

$$\text{Water uptake} = \frac{(W_w - W_d)}{W_d} \times 100\% \quad (6)$$

Ion exchange capacity (IEC) is characterized using acid-base titration with NaCl media. A membrane with a size of 2×2 cm^2 was immersed in HCl 0.1 M solution for 24 h. The membrane in the form of H^+ was converted

into Na^+ by soaking in NaCl 1 M for 24 h. Then, the removed H^+ was titrated with NaOH 0.01 M using the phenolphthalein indicator. IEC was measured using Eq. (7) [18].

$$IEC = \frac{(M \times V)_{NaOH}}{W_d} \quad (7)$$

Electrochemical impedance spectroscopy (EUGOL U2826) was used to analyze the conductivity of the membrane. The membrane was clamped using Cu electrodes and tested at room temperature in the 20 Hz–5 MHz frequency range. The value of membrane conductivity (σ) was measured using Eq. (8) [23];

$$\sigma = \frac{l}{R \times A} \quad (8)$$

where l is membrane thickness (cm), R is resistance (Ω), and A is probe area (cm^2).

■ RESULTS AND DISCUSSION

Isolation and Sulfonation of Lignin OPEFB

Analysis of lignin and lignosulfonate was carried out using FTIR. The shift of wavenumber and the peak of new uptake that exists in the isolation results showed in Fig. 1. Based on the spectra, it can be seen that the peak at the wavenumber 3387, 2931, and 1240 cm^{-1} indicates the presence of an O–H, C–H, and aromatic C=C bond respectively. This result aligns with the previous report [24] in Table 2. Sulfonation using sodium sulfite showed an absorption peak at 1192, 1663, and 1540 cm^{-1}, which indicates the sulfonate group, OH, and CH_3 groups following previous research [25-27]. Spectra of lignosulfonate appear in Fig. 2.

The sulfonation degree of lignin and lignosulfonate is characterized using conductometric titration. Table 3 shows the increasing sulfonate content at the material filler. The sulfonation degree increased by 8.9% in the lignosulfonate. Sulfonation occurs through the substitution of a sulfonate group on the aliphatic hydroxyl group of lignin through an addition reaction,

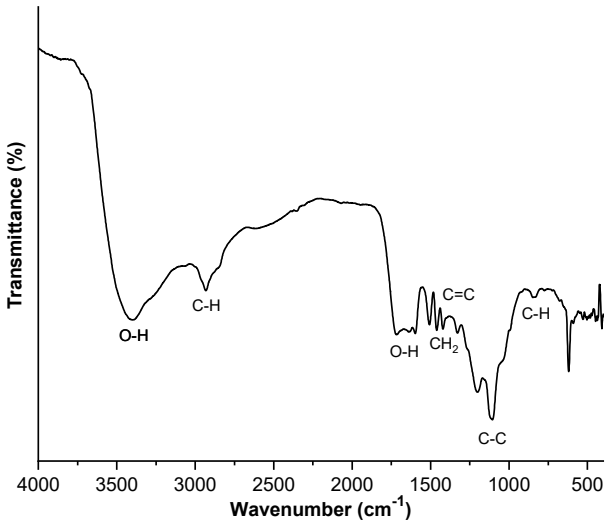

Fig 1. FTIR spectra of lignin OPEFB

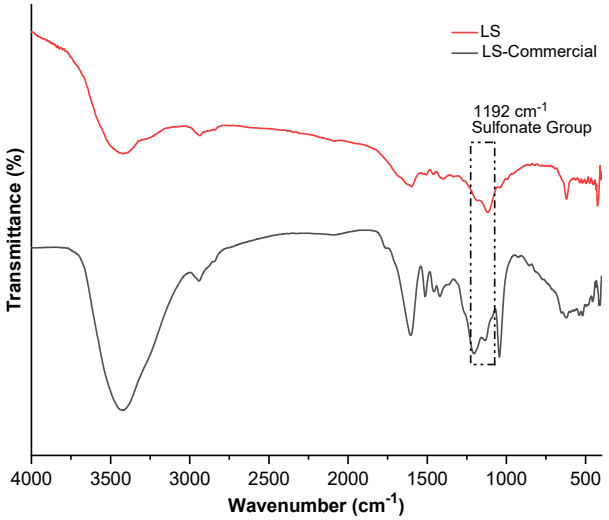

Fig 2. FTIR spectra of lignosulfonate

Table 2. Lignin FTIR uptake peaks

Absorption	Wavenumber (cm^{-1})	Wavenumber (cm^{-1}) [24]
O–H stretching	3387	3322
C–H stretching	2931	2918
O–H deformation	1597	1593
$-CH_2$ deformation	1420	1420
Aromatic C=C	1240	1238
C–C stretching	1030	1027
C–H deformation	899	895

Table 3. Sulfonation degree of lignin and lignosulfonate

Material	Sulfonation degree (mmol/g)
Lignin	1.35
Lignosulfonate	1.47

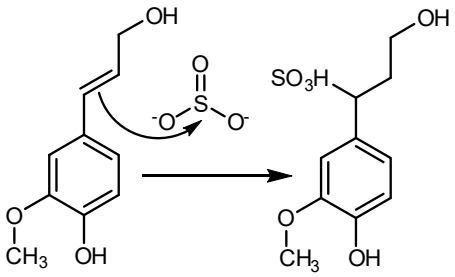

Fig 3. Lignin sulfonation mechanism [28]

as shown in Fig. 3. Sulfite reacts with the carbon double bond at the alpha position [28].

Lignin thermally decomposed in a large range of temperatures because of various functional groups that attached have different thermal stability. The differences in the structure and chemical nature of lignin from different sources could account for the diversity of its degradation behavior [29]. From Fig. 4, it can be seen that lignin begins to degrade at the temperature of 250 °C and ends at 776 °C. At this temperature, propanoid side chains such as methyl-, ethyl, vinyl guaiacol, and the main aromatic structure of lignin began to decompose [30]. While for lignosulfonate, degradation occurs in three stages at temperatures of 29, 408, and 611 °C. The first degradation below 100 °C can be mainly attributed to the loss of moisture [29]. The higher temperature of main structure degradation that occurs above 408 °C can be caused due to cross-link between lignin on sulfonate bonds that need more energy to degrade [31]. The last degradation that occurs at a temperature above 500 °C possibly related to the slow decomposition of some aromatic rings in the lignosulfonate [29]. The data indicate that lignosulfonate has higher thermal stability than lignin.

Membrane PVDF/Lignin and PVDF/Lignosulfonate

The membrane was prepared by phase inversion, and the result is presented in Fig. 5. The addition of lignin and lignosulfonate affect the color and homogeneity of the membranes. The addition of lignin gives a deeper yellow color with increasing filler concentration. In PLS

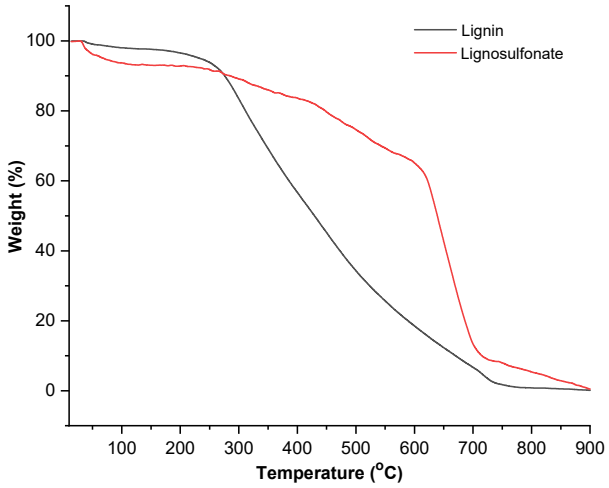

Fig 4. Diffractogram TGA of lignin and lignosulfonate

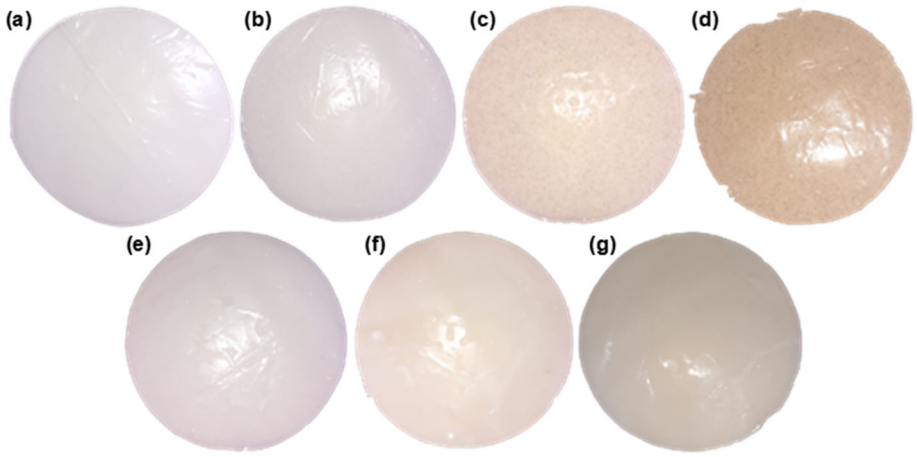

Fig 5. The photograph of membrane (a) PVDF, (b) PL-1, (c) PL-3, (d) PL-5, (e) PLS-1, (f) PLS-3, and (g) PLS-5

membranes, homogeneity is formed better, making that membrane surface more transparent than the PL membrane. The presence of cross-link in the lignosulfonate reduces hydrophilicity that makes well interact with the PVDF and solvent, resulting more homogenous membrane.

Membrane Morphology

In Fig. 6, membrane PVDF has a tight surface. The addition of lignin and lignosulfonate makes the membrane surface rougher. Fig. 6 also shows the cross-section membrane. It can be seen that all the membranes have an asymmetric structure with finger-like and sponge-like pores. PVDF membrane has a shorter finger-like and thicker sponge-like area than PL and PLS. When the phase inversion occurs, the solvent is rapidly transferred to the water, forming finger-like pores. However, solvent migration occurs slowly at the lower area and leaves a sponge-like pore structure. The hydroxyl group from lignin and lignosulfonate attracts more water at PL and PLS membranes and affects the speed of solvent migration, producing longer finger-like pores.

Membranes Thermal Analysis

Fig. 7 shows the thermogram TGA of the PVDF, PL, and PLS membranes. Degradation of the membrane occurs at temperatures of 432–760 °C with two stages of degradation. Thermal degradation of all samples was similar, caused by weak interaction between filler and PVDF matrix. This suggests that the addition of filler did not change the degradation mechanism of PVDF membrane [32]. On the membrane, the first stage of degradation occurs at 432 °C that related to the decomposition of hydrogen and fluorine from the main chain of the PVDF structure [33]. The second stage at above 480 °C indicates the degradation of PVDF backbone [34].

Mechanical Properties

The mechanical properties of polymer electrolyte membranes with the addition of lignin and lignosulfonate are shown in Table 4. At the PVDF membrane, tensile strength reaches 4.8 MPa with an elongation of 93% and

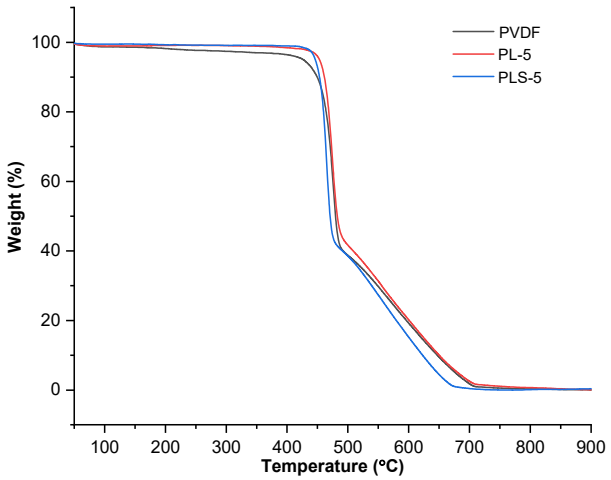

Fig 7. Thermogram TGA of PVDF, PL, and PLS membranes

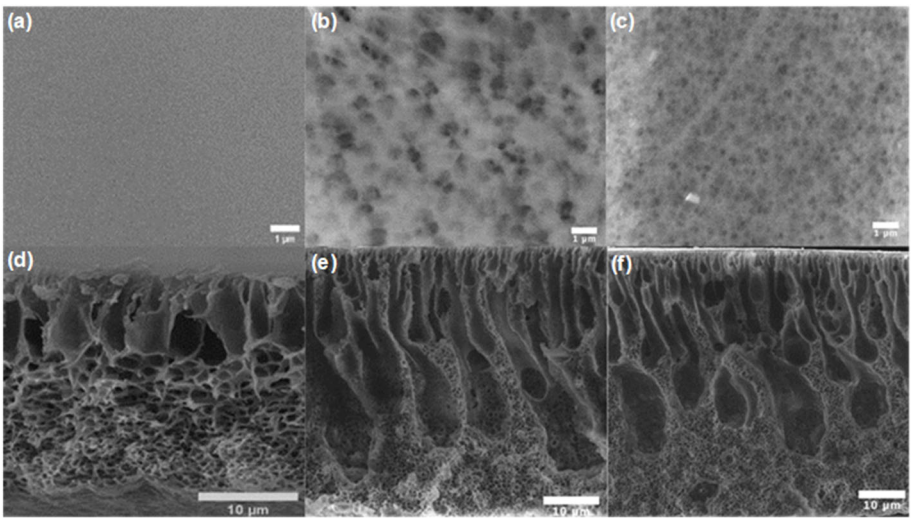

Fig 6. Surface and cross-section morphology of (a,d) PVDF, (b,e) PL-5, and (c,f) PLS-5

Table 4. Mechanical properties of the membranes

Membrane	l (mm)	σ at break (MPa)	ε at break (%)	γ (MPa)
PVDF	0.05	4.80	93.30	16.60
PL-1	0.07	2.80	60.00	17.50
PL-3	0.05	2.90	76.70	31.40
PL-5	0.05	2.50	56.70	22.20
PLS-1	0.05	4.80	86.70	60.10
PLS-3	0.07	3.40	66.70	16.60
PLS-5	0.06	3.60	80.00	37.00

a low young modulus of 16.6 MPa. In general, the addition of lignin or lignosulfonate reduces the value of tensile strength and elongation but increases the young modulus. These mechanical properties show that the membrane becomes more brittle than pure PVDF membrane. This can be caused by the presence of polar groups and aromatic rings, which make the membrane more rigid. Good dispersion also affects the mechanical properties of membranes [35]. With lignin addition, the membrane has a poor homogeneity caused by different polarities between the hydrophobic PVDF and hydrophilic side of lignin. This results in a big decrease in tensile strength and elongation by 42%. While with lignosulfonate filler, PVDF forms a homogeneous membrane and fewer pores that resulted in less decrease in mechanical strength.

Matrix Structure and Membrane Hydrophilicity

The matrix structure of membranes was observed using XRD and ATR-FTIR. Fig. 8 reveals the peaks at 2θ of 18.39°, 23.75°, and 21.35°, which correspond to α and β phases of PVDF, respectively [36-37]. At the peak of 18.39° and 23.75°, PVDF membranes have a relatively higher intensity than PL or PLS, which indicates a decrease in the α phase. The addition of lignin or lignosulfonate increases the intensity of the peak at 21.35° related to polyethylene-like structure, which indicate β phase.

ATR-FTIR spectra in Fig. 9 showed the presence of α and β phases that supported XRD data. β phase was observed at 840 cm^{-1}, which is stretching asymmetry of CF_2 [38] while the peak at 762 cm^{-1} is CF_2 bending of α phase [39]. Based on Fig. 9, it can be seen that intensity of the β phase for PL and PLS increases meanwhile the α phase is reduced. The higher β phase intensity means that

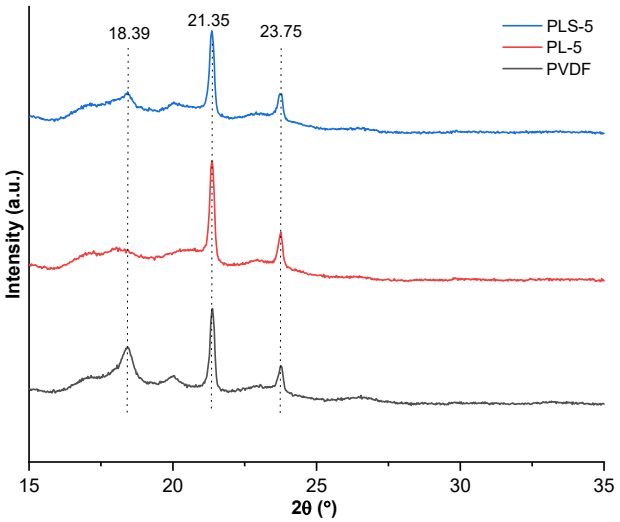

Fig 8. Diffractogram XRD of PVDF, PL-5, and PLS-5 membranes

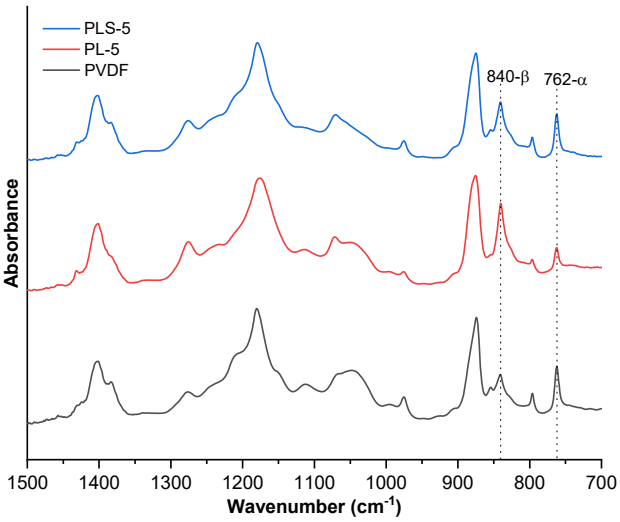

Fig 9. Membranes ATR-FTIR spectra

more hydrophilic membranes are formed [40]. β fraction of the membrane PVDF increased from 40.6 to 60.2% and 49.5% in PL and PLS, respectively. This suggests that lignin is more significant in increasing the hydrophilicity value of the membrane.

Surface hydrophilicity was also analyzed using a water contact angle and the data shown in Fig. 10. PVDF membrane has a contact angle of 74.7° while the addition of filler, the contact angle decreases, which means the hydrophilicity increased. The membrane PL-5 has the lowest water contact angle of 57.9° while for lignosulfonate addition contact angle decrease to 66.7° for PLS-1. This data is supported by the β fraction that shows PL is more hydrophilic than PLS membrane.

Water Uptake, Ion Exchange Capacity, and Conductivity of Membranes

The water uptake value indicates the membrane's ability to absorb and transport water, while the IEC represents the number of cations that can be exchanged with protons. The water uptake data are shown in Fig. 11. Water uptake increase with a higher concentration of lignin or lignosulfonate due to the hydrophile group attached to the membrane.

Fig. 12 shows the IEC value on the membrane has increased along with the high concentration of lignin and lignosulfonate. The addition of lignosulfonate resulted in a higher IEC value than the addition of lignin because the presence of sulfonate groups resulted in the

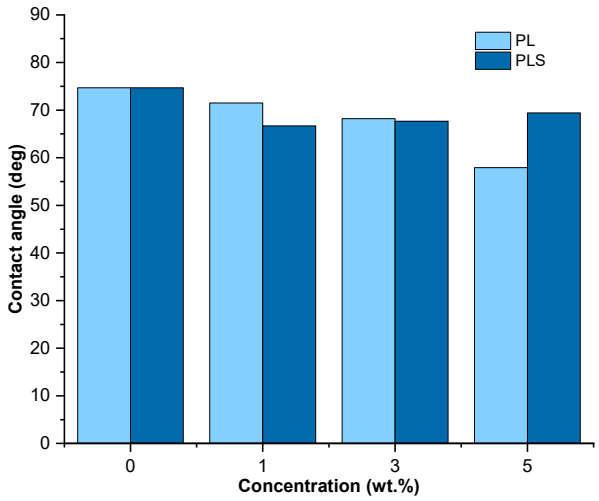

Fig 10. Membrane water contact angle

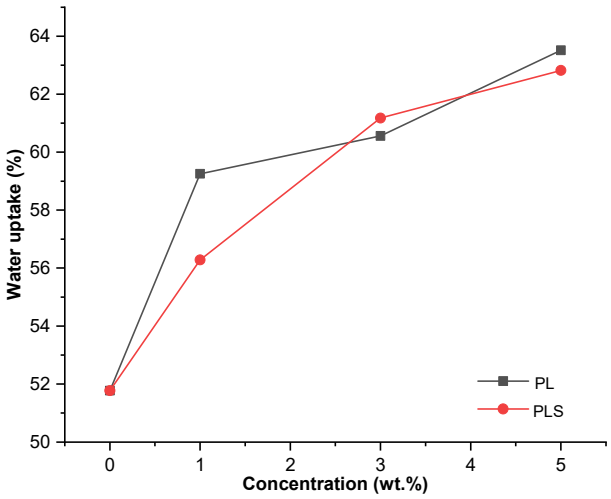

Fig 11. Membrane water uptake

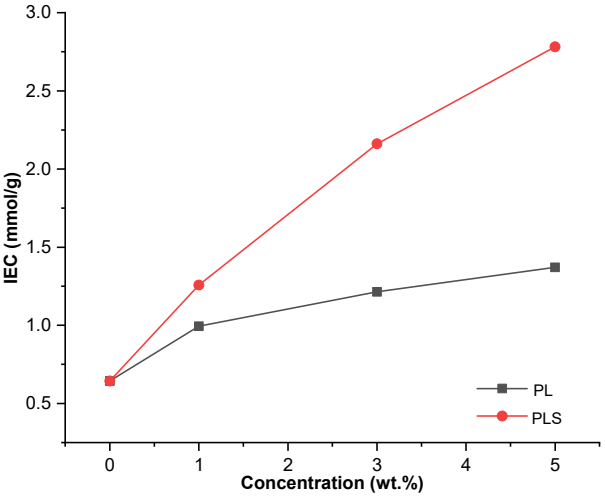

Fig 12. Membrane ion exchange capacity

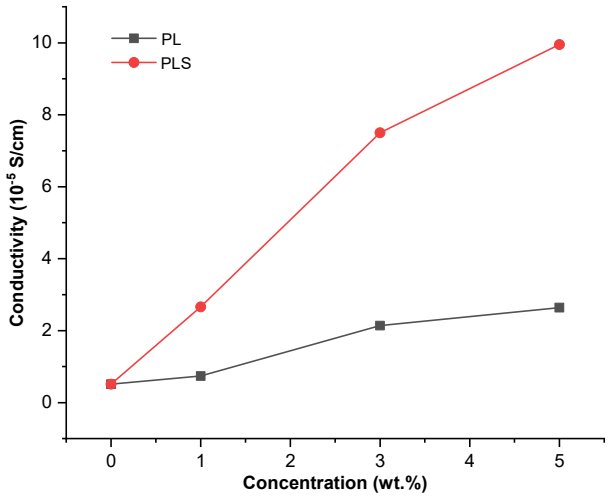

Fig 13. Membrane ionic conductivity

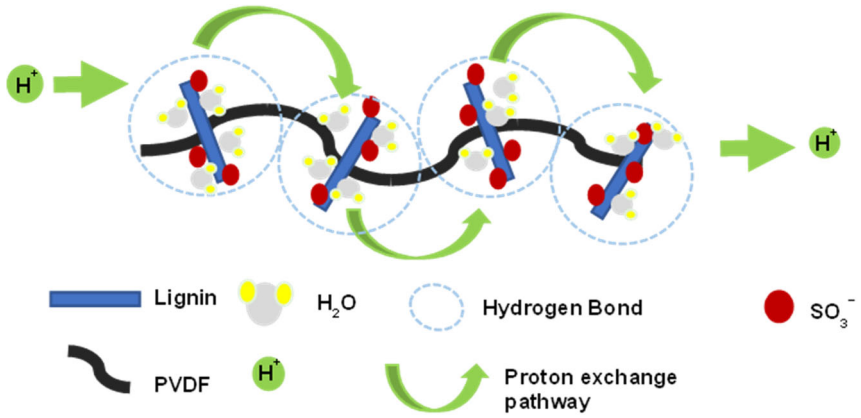

Fig 14. Proton transport mechanism

presence of sites in ion exchange. Membrane PLS-5 with an IEC of 2.78 mmol/g has a higher value than the Nafion® 117 polymer which only 0.91 mmol/g [41].

Ionic conductivity increases with increasing filler concentration as shown in Fig. 13. From the data, PVDF membrane has 0.51×10^{-5} S/cm and increase up to 9.95×10^{-5} S/cm for 5% lignosulfonate addition. This data is linear with IEC because IEC affects the ionic conductivity of the membrane [38-39]. The presence of sulfonate groups helps in the process of ion transfer. The proton transport mechanism via the Grotuss mechanism is shown in Fig. 14. Proton transportation occurs because of the protonation and deprotonation of hydrogen bonds [42]. Proton jumps between adjacent sulfonic acid groups or water molecules to achieve proton transfer [43]. In PLS-5, conductivity increases due to greater water uptake and IEC, where sulfonic facilitated proton transport from anode to cathode [44].

■ CONCLUSION

Isolation and sulfonation of lignin from OPEFB were successfully carried out. Adding lignin and lignosulfonate fillers affects membrane morphology, thermal, mechanical, matrix structure, hydrophilicity, and water uptake. Membranes have asymmetric structures with finger-like and sponge-like pores. All the membrane has similar degradation temperature caused by weak interaction between filler and PVDF matrix. The mechanical properties decreased with the addition of filler, while the surface hydrophilicity and water uptake increased. Membrane matrix composed of α and β phase. The β phase intensity increase with the addition of lignin and lignosulfonate. The ion exchange capacity and ionic conductivity also showed a high increase of 2.78 mmol/g and 9.95×10^{-5} S/cm, respectively. Based on the data obtained, it shows that the membrane PVDF modified with lignosulfonate has the potential as a polymer electrolyte membrane.

■ ACKNOWLEDGMENTS

The authors thank *Badan Pengelolaan Dana Perkebunan Kelapa Sawit* (BPDPKS) as the research funder of *Riset Sawit Mahasiswa 2022* No. PENG-2/DPKS.4/2022 and also to the Chemistry Laboratory UNS for facilitating the research to completion.

■ AUTHOR CONTRIBUTIONS

Nala Ridhwanul Mu'izzah and Pinka Zuhdiana Hapsari conducted the experiment and wrote the manuscript. Nabila Putri Aulia, Dian Wahyu Tri Wulansari, and Fauziyah Azhari do the analysis and reviewing. Edi Pramono supervised and review the manuscript. All authors agreed to the final version of this manuscript.

■ REFERENCES

[1] Abeleda Jr, J.M.A., and Espiritu, R., 2022, The status and prospects of hydrogen and fuel cell technology in the Philippines, *Energy Policy*, 162, 112781.

[2] Sokmez, E., Taymaz, I., and Kahveci, E.E., 2022, Performance evaluation of direct ethanol fuel cell using a three-dimensional CFD model, *Fuel*, 313, 123022.

[3] Nicolay, S., Karpuk, S., Liu, Y., and Elham, A., 2021, Conceptual design and optimization of a general aviation aircraft with fuel cells and hydrogen, *Int. J. Hydrogen Energy*, 46 (64), 32676–32694.

[4] Perčić, M., Vladimir, N., Jovanović, I., and Koričan, M., 2022, Application of fuel cells with zero-carbon fuels in short-sea shipping, *Appl. Energy*, 309, 118463.

[5] Ferraren-De Cagalitan, D.D.T., and Abundo, M.L.S., 2021, A review of biohydrogen production technology for application towards hydrogen fuel cells, *Renewable Sustainable Energy Rev.*, 151, 111413.

[6] Sigwadi, R., Dhlamini, M.S., Mokrani, T., Ṋemavhola, F., Nonjola, P.F., and Msomi, P.F., 2019, The proton conductivity and mechanical properties of Nafion®/ ZrP nanocomposite membrane, *Heliyon*, 5 (8), e02240.

[7] Bose, S., Kuila, T., Nguyen, T.X.H., Kim, N.H., Lau, K.T., and Lee, J.H., 2011, Polymer membranes for high temperature proton exchange membrane fuel cell: Recent advances and challenges, *Prog. Polym. Sci.*, 36 (6), 813–843.

[8] Ayyubi, S.N., and Admaja, L., 2020, Pengaruh variasi konsentrasi montmorillonit terhadap sifat dan kinerja membran kitosan/PVA/MMT untuk aplikasi DMFC, *Walisongo J. Chem.*, 3 (1), 1–9.

[9] Silitonga, R.S., Widiastuti, N., Jaafar, J., Ismail, A.F., Abidin, M.N.Z., Azelee, I.W., and Naidu, M., 2018, The modification of PVDF membrane via cross-linking with chitosan and glutaraldehyde as the cross-linking agent, *Indones. J. Chem.*, 18 (1), 1–6.

[10] Dyartanti, E.R., Purwanto, A., Widiasa, I.N., and Susanto, H., 2018, Ionic conductivity and cycling stability improvement of PVDF/nano-clay using PVP as polymer electrolyte membranes for $LiFePo_4$ batteries, *Membranes*, 8 (3), 36.

[11] Abriyanto, H., 2021, Hydrophilic modification of PVDF membrane: A review, *JMM*, 1 (1), 1–9.

[12] Lu, J., Cheng, M., Zhao, C., Li, B., Peng, H., Zhang, Y., Shao, Q., and Hassan, M., 2022, Application of lignin in preparation of slow-release fertilizer: Current status and future perspectives, *Ind. Crops Prod.*, 176, 114267.

[13] Liu, Y., Mao, X., Wu, H., Wang, X., Shi, B., Fan, C., Kong, Y., and Jiang, Z., 2022, Sulfonated lignin intercalated graphene oxide membranes for efficient proton conduction, *J. Membr. Sci.*, 644, 120126.

[14] Lupatini, K.N., Schaffer, J.V., Machado, B., Silva, E.S., Ellendersen, L.S.N., Muniz, G.I.B., Ferracin, R.J., and Alves, H.J., 2018, Development of chitosan membranes as a potential PEMFC electrolyte, *J. Polym. Environ.*, 26 (7), 2964–2972.

[15] Ganguly, P., Sengupta, S., Das, P., and Bhowal, A., 2020, Valorization of food waste: Extraction of cellulose, lignin and their application in energy use and water treatment, *Fuel*, 280, 118581.

[16] Fatriasari, W., Ulwan, W., Aminingsih, T., Sari, F.P., Fitria, F., Suryanegara, L., Iswanto, A.H., Ghozali, M., Kholida, L.N., Hussin, M.H., Fudholi, A., and Hermiati, E., 2021, Optimization of maleic acid pretreatment of oil palm empty fruit bunches (OPEFB) using response surface methodology to produce reducing sugars, *Ind. Crops Prod.*, 171, 113971.

[17] Zakaria, N.A., Hazwan Hussin, M., Ahmad, A.L., Leo, C.P., Poh, P.E., Behzadian, K., Akinwumi, I.I., Moghayedi, A., and Diazsolano, J., 2021, Lignin modified PVDF membrane with antifouling properties for oil filtration, *J. Water Process Eng.*, 43, 102248.

[18] Ye, J., Cheng, Y., Sun, L., Ding, M., Wu, C., Yuan, D., Zhao, X., Xiang, C., and Jia, C., 2019, A green SPEEK/lignin composite membrane with high ion selectivity for vanadium redox flow battery, *J. Membr. Sci.*, 572, 110–118.

[19] Setiati, R., Siregar, S., and Wahyuningrum, D., 2020, "Laboratory Optimization Study of Sulfonation Reaction toward Lignin Isolated from Bagasse" in *Biotechnological Applications of Biomass*, Eds., Basso, T.P., Basso, T.O., and Basso, L.C., IntechOpen, Rijeka, Croatia.

[20] Rocha, I., Ferraz, N., Mihranyan, A., Strømme, M., and Lindh, J., 2018, Sulfonated nanocellulose beads as potential immunosorbents, *Cellulose*, 25 (3), 1899–1910.

[21] Bărdacă Urducea, C., Nechifor, A.C., Dimulescu, I.A., Oprea, O., Nechifor, G., Totu, E.E., Isildak, I., Albu, P.C., and Bungău, S.G., 2020, Control of

nanostructured polysulfone membrane preparation by phase inversion method, *Nanomaterials*, 10 (12), 2349.

[22] He, Z., Rault, F., Vishwakarma, A., Mohsenzadeh, E., and Salaün, F., 2022, High-aligned PVDF nanofibers with a high electroactive phase prepared by systematically optimizing the solution property and process parameters of electrospinning, *Coatings*, 12 (9), 1310.

[23] Grewal, M.S., Kisu, K., Orimo, S., and Yabu, H., 2022, Increasing the ionic conductivity and lithium-ion transport of photo-cross-linked polymer with hexagonal arranged porous film hybrids, *iScience*, 25 (9), 104910.

[24] Pradana, M.A., Ardhyananta, H., and Farid, M., 2017, Pemisahan selulosa dari lignin serat tandan kosong kelapa sawit dengan proses alkalisasi untuk penguat bahan komposit penyerap suara, *Jurnal Teknik ITS*, 6 (2), 413–416.

[25] Ganie, K., Manan, M.A., Ibrahim, A., and Idris, A.K., 2019, An Experimental approach to formulate lignin-based surfactant for enhanced oil recovery, *Int. J. Chem. Eng.*, 2019, 4120859.

[26] Ismiyati, I., Suryani, A., Mangunwidjaya, D., Machfud, M., and Hambali, E., 2009, Pembuatan natrium lignosulfonat berbahan dasar lignin isolat tandan kosong kelapa sawit: Identifikasi, dan uji kinerjanya sebagai bahan pendispersi, *J. Tek. Ind. Pert.*, 19 (1), 25–29.

[27] Karimov, O.K., Teptereva, G.A., Chetvertneva, I.A., Movsumzade, E.M., and Karimov, E.K., 2021, The structure of lignosulfonates for production of carbon catalyst support, *IOP Conf. Ser.: Earth Environ. Sci.*, 839, 022086.

[28] Eraghi Kazzaz, A., Hosseinpour Feizi, Z., and Fatehi, P., 2019, Grafting strategies for hydroxy groups of lignin for producing materials, *Green Chem.*, 21 (21), 5714–5752.

[29] Poletto, M., 2017, Assessment of the thermal behavior of lignins from softwood and hardwood species, *Maderas: Cienc. Tecnol.*, 19 (1), 63–74.

[30] Ramezani, N., and Sain, M., 2018, Thermal and physiochemical characterization of lignin extracted from wheat straw by organosolv process, *J. Polym. Environ.*, 26 (7), 3109–3116.

[31] Montoya-Ospina, M.C., Verhoogt, H., Ordner, M., Tan, X., and Osswald, T.A., 2022, Effect of cross-linking on the mechanical properties, degree of crystallinity and thermal stability of polyethylene vitrimers, *Polym. Eng. Sci.*, 62 (12), 4203–4213.

[32] Yi, G., Li, J., Henderson, L.C., Lei, W., Du, L., and Zhao, S., 2022, Enhancing thermal conductivity of polyvinylidene fluoride composites by carbon fiber: Length effect of the filler, *Polymers*, 14 (21), 4599.

[33] Lusiana, R.A., Indra, A., Prasetya, N.B.A., Sasongko, N.A., Siahaan, P., Azmiyawati, C., Wijayanti, N., Wijaya, A.R., and Othman, M.H.D., 2021, The effect of temperature, sulfonation, and PEG addition on physicochemical characteristics of PVDF membranes and its application on hemodialysis membrane, *Indones. J. Chem.*, 21 (4), 942–953.

[34] Li, W., Li, H., and Zhang, Y.M., 2009, Preparation and investigation of PVDF/PMMA/TiO_2 composite film, *J. Mater. Sci.*, 44 (11), 2977–2984.

[35] de Menezes, B.R.C., Ferreira, F.V., Silva, B.C., Simonetti, E.A.N., Bastos, T.M., Cividanes, L.S., and Thim, G.P., 2018, Effects of octadecylamine functionalization of carbon nanotubes on dispersion, polarity, and mechanical properties of CNT/HDPE nanocomposites, *J. Mater. Sci.*, 53 (20), 14311–14327.

[36] Gao, M., Zhu, Y., Yan, J., Wu, W., and Wang, B., 2022, Micromechanism study of molecular compatibility of PVDF/PEI blend membrane, *Membranes*, 12 (8), 809.

[37] Bai, H., Wang, X., Zhou, Y., and Zhang, L., 2012, Preparation and characterization of poly(vinylidene fluoride) composite membranes blended with nano-crystalline cellulose, *Prog. Nat. Sci.: Mater. Int.*, 22 (3), 250–257.

[38] Sui, Y., Chen, W.T., Ma, J.J., Hu, R.H., and Liu, D.S., 2016, Enhanced dielectric and ferroelectric properties in PVDF composite flexible films through doping with diisopropylammonium bromide, *RSC Adv.*, 6 (9), 7364–7369.

[39] Cai, X., Lei, T., Sun, D., and Lin, L., 2017, A critical analysis of the α, β and γ phases in poly(vinylidene fluoride) using FTIR, *RSC Adv.*, 7 (25), 15382–15389.

[40] Teoh, G.H., Ooi, B.S., Jawad, Z.A., dan Low, S.C., 2021, Impacts of PVDF polymorphism and surface printing micro-roughness on superhydrophobic membrane to desalinate high saline water, *J. Environ. Chem. Eng.*, 9 (4), 105418.

[41] Espiritu, R., Mamlouk, M., and Scott, K., 2016, Study on the effect of the degree of grafting on the performance of polyethylene-based anion exchange membrane for fuel cell application, *Int. J. Hydrogen Energy*, 41 (2), 1120–1133.

[42] Wang, M., Wang, L., Deng, N., Wang, X., Xiang, H., Cheng, B., and Kang, W., 2021, Electrospun multi-scale nanofiber network: Hierarchical proton-conducting channels in Nafion composite proton exchange membranes, *Cellulose*, 28 (10), 6567–6585.

[43] Zhai, S., Dai, W., Lin, J., He, S., Zhang, B., and Chen, L., 2019, Enhanced proton conductivity in sulfonated poly(ether ether ketone) membranes by incorporating sodium dodecyl benzene sulfonate, *Polymers*, 11 (2), 203.

[44] Lee, K.H., Chu, J.Y., Kim, A.R., and Yoo, D.J., 2019, Effect of functionalized SiO_2 toward proton conductivity of composite membranes for PEMFC application, *Int. J. Energy Res.*, 43 (10), 5333–5345.